Eurographics Italian Chapter Conference (2006)
G. Gallo and S. Battiato and F. Stanco (Editors)

Shape Reconstruction with Uncertainty

L. Papaleo†, E. Puppo

Department of Informatics and Computer Science, University of Genova, Italy

Abstract

This paper presents a general Surface Reconstruction framework which encapsulates the uncertainty of the sampled data, making no assumption on the shape of the surface to be reconstructed. Starting from the input points (either points clouds or multiple range images), an Estimated Existence Function (EEF) is built which models the space in which the desired surface could exist and, by the extraction of EEF critical points, the surface is reconstructed. The final goal is the development of a generic framework able to adapt the result to different kinds of additional information coming from multiple sensors.

Categories and Subject Descriptors (according to ACM CCS): I.3.3 [Computer Graphics]: Shape Modeling, Uncertain data, Multi-sensor Data Fusion

1. Introduction

3D scanning devices are becoming more and more available and affordable. Thanks to modern acquisition technologies, heterogeneous data can be acquired from multiple acquisition sensors, which often incorporate information about uncertainty of the data sampling process. Surface reconstruction techniques designed over a specific sensor often take into account uncertainty during the reconstruction process, but they are limited to work with a single device. On the contrary, general techniques that can process data coming from different sensors usually disregard much part of sensor-specific information, and seldom take into account uncertainty.

The basic concept of our approach is *uncertainty*: lack of knowledge, which cannot be predicted and may be caused, e.g. from inadequate model etc. In case of multiple acquisition technologies, there are different types of uncertainty:

- Incompleteness: sensors possibly leave something out.
- Imprecision: sensors can provide only approximate information.
- Inconsistency: sensors data may not always agree with each other.
- Ambiguity: data from various sensors may be indistinguishable from one another.

The goal of our research is to define a flexible technique that can deal with data coming from different sensors, while it fully exploits specific information about uncertainty associated to each specific sensor. To this aim, we adopt a probabilistic approach. We use information attached to data samples to define and generate an *Estimated Existence Function* (EEF), which represents the probability that the desired surface exists in a volume of space. The reconstructed surface is then extracted by considering the ridges of our EEF and building a triangle mesh out of them.

Each sample point in the input dataset brings information about the surface in its neighborhood. Information available for a single point may go from the bare coordinates, to estimation of differential properties like surface normal or curvature, to more or less elaborate estimation of uncertainty. On the basis of such information, different probability distribution functions may be obtained, which shape the contribution of each sampled point to define the EEF in its neighborhood. Under the assumption that all samples are independent, the EEF is built by combining contributions coming from the different samples.

In this preliminary work, we analyze a simple scenario: each sample consists just of the coordinates of a point in space, plus an estimation of uncertainty in the form of a scalar value. Under this assumption, we adopt a Gaussian distribution to model our EEF. We present some results on both synthetic and real datasets.

† Corresponding author. papaleo@disi.unige.it

2. Related Work

A burst of research has been made during the last decade on 3D Reconstruction and several interesting and well-behaved algorithms have been developed. General solutions should not assume any knowledge of the object shape or topology but possible approaches may strongly depend on the given type of input (e.g. point clouds, multiple range images). It is not simple to propose a significant taxonomy of the existing surface reconstruction methods: most of them, especially in the last few years, try to adopt hybrid solutions using different approaches in the same method. Regardless the underlying structure of data, approaches can be divided into two groups [MM98], depending on whether they produce an interpolation or an approximation of the input data.
The interpolating approaches, in some sense, rely on the accuracy of the input and use them as constraints for the construction of the final mesh [ACTL02, Att97, AS00, BBCS96, TGLW01, HDD*92, TC98]. The basic strategy is to use the input points as the optimal geometric description of the scanned object. In general, a cloud of points with no other information is considered [BBCS96, TGLW01]. In some cases, also point clouds with additional information on the object structure or proximity of points maybe processed [ACTL02, Att97, AS00]. In addition, the modern scanning technologies often return also an estimation of the normal in each point that can be used [TC98]. In case of approximation methods, the vertices in the resulting mesh can be different from the original sampled points. The basic strategy is to use input points as a *guide* for surface reconstruction. Especially for range data, an approximating rather than an interpolating mesh is desirable in order to get a result of moderate complexity [CM95, CMSR00, CL96, HSIW96, JM02].

Few recent existing approaches try to consider the confidence of the sampled data. Schneider analyzed shape uncertainty from a more abstract point of view in [Sch01]. He identifies various sources for shape uncertainty and stresses the importance of additional context information to reduce the uncertainty. Guibas et al. [PMG04] try to describe shape information by combining local estimates using influence functions. Part of our work is most closely related to the one presented by Johnson and Manduchi [JM02]. Both of them use a probabilistic rule for constructing a probability function. The scope of their work is quite different though, since they mainly concentrate on terrains by the use of radar input datasets.

3. Problem Definition and proposed approach

From a mathematical point of view, the surface of a 3D object can be defined as a two-dimensional manifold that is compact, orientable and connected. Our Surface Reconstruction problem can be formalized as follow:

> Given a set of measurements $V = \{\mu_1, \ldots, \mu_n\}$ of an object (environment), coming from different sensors $s_1, \ldots, s_k$ and a set of additional information $M = \{M_1, \ldots, M_n\}$ related to the given measurements in V, find a surface $S \subset \Re^3$ that approximates the observed object.

Each M_i may contain properties related to the measurement i (e.g., RGB color of the measurement, geometric properties such as normal vector and local curvature) or measurement models (i.e, an error model, a reliability model, and so on).

Our idea is to define a *Probability Density Function* (PDF for short) for each measurement μ_i integrating all the information present in the M_i. The PDF will indicate the degree of *importance* of μ_i in the reconstruction process of the desired surface F. The PDFs related to measurements, support the construction of the *Estimated Existence Function* (*EEF* for short) and for building it, we define:

- U_x a suitable neighborhood of a point x with $x \in \Re^3$
- $P(\mu \text{ is } x)$ as the probability that μ measures a point in U_x
- $P(x \in S)$ as $P(S \cap U_x \neq \emptyset)$

The probability P that, given a measurement μ, a point x is on the desired surface S of the observed object is

$$\begin{aligned} P(x \in S|\mu) &= P(x \in S|\mu \text{ is } x) \cdot P(\mu \text{ is } x) \\ &+ P(x \in S|\overline{\mu \text{ is } x}) \cdot \overline{P(\mu \text{ is } x)} \end{aligned}$$

If all the measurements come exactly from the surface, then the probability that a given x measures the surface S at x is obviously 1 (maximum of information). If we have a generic point x and no measurements on it, we cannot infer anything on x. In this case, we adopt a conventional probability of $\frac{1}{2}$ (minimum of information on x). Additionally, we have that $\overline{P(\mu \text{ is } x)} = 1 - P(\mu \text{ is } x)$ and from the equation above:

$$P(x \in S|\mu) = 1 \cdot P(\mu \text{ is } x) + \frac{1}{2} \cdot (1 - P(\mu \text{ is } x)) \quad (1)$$

$$P(x \in S|\mu) = \frac{1}{2} \cdot (1 + M_\mu(x)) \quad (2)$$

where M_μ is the measurement model related to the measurement μ. Equation 2 shows that if the point x falls within the measurement model, then the surface probability will be greater than $\frac{1}{2}$ but less than 1; otherwise the probability is $\frac{1}{2}$. Also, given μ, the probability P that a point x lies on the surface S is directly proportional to the value of the measurement model M_μ computed on x. Given the input dataset in the form of n independent measurements $\{\mu_1, \ldots, \mu_n\}$, the *Estimated Existence Function* of a point x in space is the probability that x lies on the desired surface S:

$$EEF(x) = P^n(x) = P(x \in S|\mu_1, \ldots, \mu_n) \quad (3)$$

Using similar reasoning as above, $P^n(x)$ can be derived from multiple independent measurement models:

$$\begin{aligned} EEF(x) &= P(x \in S|\mu_i \text{ is } x, \text{ all } i) \cdot P(\mu_i \text{ is } x, \text{ all } i) \\ &+ P(x \in S|\overline{\mu_i \text{ is } x, \text{ all } i}) \cdot \overline{P(\mu_i \text{ is } x, \text{ all } i)} \end{aligned}$$

using the above formulas we obtain:

$$EEF(x) = 1 - \frac{1}{2}\overline{P(\mu_i \text{ is } x, \text{ all } i)} \quad (4)$$

$$= 1 - \frac{1}{2}\Pi_{i=1}^{n}(1 - P(\mu_i \text{ is } x)) \quad (5)$$

So we have:

$$P(\mu_i \text{ is } x) = \int_{U_x} M_\mu(y), dy \quad (6)$$

In cases of small U_x for each x, we can approximate the integral as follows:

$$P(\mu_i \text{ is } x) = \int_{U_x} M_\mu(y), dy \cong M_\mu(x)|U_x| \equiv E^i(x) \quad (7)$$

Where $|U_x|$ is the volume of U_x. From equation 5, substituting symbols using equation 7 we can define:

$$EEF(x) = P^n(x) = 1 - \frac{1}{2}\Pi_{i=1}^{n}(1 - P(\mu_i \text{ is } x)) \quad (8)$$

$$= 1 - \frac{1}{2}\Pi_{i=1}^{n}(1 - E^i(x)) \quad (9)$$

Equation 9 indicates our **Estimated Existence Function** for each point in space and how it depends on all the models $M_i \in M$ related to all the measurements $\mu \in V$.

Once we have defined the EEF, we search for the *characteristic points* of the EEF, following the definition of Eberly et al. of surface ridges on a volume [EGM*94]. Basically, a point x is a **ridge point of type** $3-1$ (surface-on-a-volume) if $\nu_1^T(x) \cdot \nabla f(x) = 0$ and $k_i(x) > 0$, where ν_i are the eigenvector of the negative Hessian matrix of f, k_i are the eigenvalues, for $i = 1,2,3$ and $\nabla f(x)$ is the gradient. The point x is a *strong* ridge point if also the property $k_1(x) > |k_3(x)|$ holds. This definition says that a point $x \in \Re^3$ is a ridge point if the component of the gradient in the maximal changing direction is zero and the function is more concave than convex. The set of points R that are ridge points of type $3-1$ identifies the surface S we are searching for.

If necessary, we can filter the set R choosing a new set $R_1 \subseteq R$ such that the points in R_1 are ridge points of type $3-1$ where the EEF function value is more than a suitable threshold θ.

$$R_1\{x \in \Re^3 | x \text{ is ridge point and } EEF(x) > \theta\} \quad (10)$$

3.1. Building the Estimated Existence Function

The definition of the Estimated Existence function is given in equation 9, under the hypothesis of n independent measurements $\mu, \ldots, \mu_n$. The independence of the measurements helps us in the definition of an *incremental rule* for the computation of the EEF which will speed-up the overall execution of the algorithm. The EEF function can be defined as

$$EEF(x) = 1 - \frac{1}{2}\Pi_{i=1}^{n}(1 - E^i(x)) = 1 - \frac{1}{2}f(x)^n \quad (11)$$

where $f(x)^n = \Pi_{i=1}^{n}(1 - E^i(x))$. So the Estimated Existence Function $EEF(x)$ depends on a function $f^n(x)$ that can be computed incrementally. In fact:

$$f^n(x) = (1 - E^i(x)) \cdot \Pi_{i=1}^{(n-1)}(1 - E^i(x)) \quad (12)$$

$$= (1 - E^i(x)) \cdot f^{n-1}(x) \quad (13)$$

The function $f^n(x)$ depends on $f^{n-1}(x)$, on the $E^i(x)$ and, as consequence, on the models $M^i(x)$ given as input for each measurement in V. In this paper, we present as model only an error measurement model related to each sampled value in the form of a *Multivariate Normal Distribution* (Gaussian Distribution).

$$G(x) = 2\pi^{\frac{n}{2}} \cdot |\Sigma|^{-\frac{1}{2}} \cdot e^{-\frac{1}{2}(x-\mu)^T \Sigma_x^{-1}(x-\mu)} \quad (14)$$

where Σ is the covariance matrix and μ is the mean vector. At this step of development, we consider only input datasets which come with a *reliability* value related to each measurement (in this case we use an isotropic Gaussian) or datasets with the covariance matrix which will be used in the Gaussian Function.

The $EEF(x)$ is defined in $\Re^3$ but for computability problem, we cannot work in the continuum. For this reason, we discretize the space using of a regular grid G with a grid step s interactively defined by the user. Moreover, for efficiency purposes, we can bound the influence space of each measurement to a certain domain without computing its contribution to the EEF over all points in $\Re^3$. From probabilistic and statistical theory [Spa99, SS95], we know that, for a Gaussian Distribution in the form of equation 14, at least $99,7\%$ of the non-zero values fall in the interval $[\mu - 3\sigma, \mu + 3\sigma]$. So we decided to compute the contribution of a measurement x to the EEF only in such a bounded portion of space. For each measurement x the inference space s_x will depend on the $3\sigma x, 3\sigma y$ and $3\sigma z$ values and can be approximated as an *ellipsoid* with principal axes depending on x, y, z.

Out of this inference space, the EEF value of a grid point will not depend on the measurement x. At this point of the process, we have a regular grid in which all points have the related EEF value: $\frac{1}{2}$ value if the grid point is not fallen in any inference space and $EEF(x)$ if it is fallen on one or more inference spaces.

4. Compute the Ridge Points

The extraction of the characteristics points of the EEF is a fundamental step for the reconstruction of the desired surface S. We have implemented two different methods: one more rigorous (and more elaborated) that follows the formal definition of characteristic surface on an approximated volume (condition by equation 10) and the other (the simplest one) that defines if a point is ridge considering the neighbours and therefore dicretizing the procedure.

4.1. Ridge surface on a volume

In order to compute the ridge points using the condition in equation 10 we need the first and second order partial deriva-

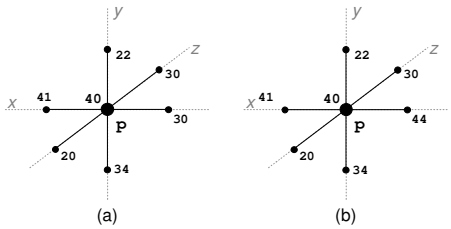

Figure 1: *(a) Point p is a ridge point. It is maximum in the z direction and not minimum in the other two. (b) Point p is not a ridge. It is maximum in the z direction but minimum in the x direction.*

tives of the EEF. While we compute the EEF value for each grid point, the derivatives can be computed following an incremental rule analogous to the one in equation 13. The partial derivatives of the EEF function will depend on the partial derivatives of $f^n(x)$. For each measurement x the system is reading, we are able to incrementally compute the EEF value and the relative first and second order partial derivatives on each influenced grid point. This effectively speeds up the entire process. Once all the partial derivatives have been computed, we use the condition in equation 10 for marking those grid points that are ridge points of type 3-1. The property of being a ridge of a grid point is an approximation: discretizing the space, we marked a grid point as ridge indicating that it is near a real ridge of the EEF function. For this reason, we added two tolerance values modifiable by the user: on the one hand, we select a subset of ridge points, filtering on the intensity value (EEF value), while on the other hand, we filter the ridge points by varying the approximation error ε (basically we test if $\nu_1(x)^T \nabla f(x) < \varepsilon$ instead of $\nu_1(x)^T \nabla f(x) = 0$).

4.2. Heuristic Method

As we said before, the heuristic method uses a less rigorous but not less effective definition of characteristic points. Considering that the EEF function is defined on a discrete domain, it is possible to study the problem from a practical point of view, as it was done in [JR75, Mar83, MB95, TF78] for the case of terrains. We have extended these techniques to 3D grids by considering the 6-adjacent neighbors of a grid point $g_{i,k,j}$, i.e. the vertices in the link of $g_{i,j,k}$ connected to $g_{i,j,k}$ through an edge [Pap04]. A grid point $g_{i,j,k}$ is a ridge if it is a local maximum in one direction (x, y, z direction) and not a minimum in the other two.
The formalization of what we have just explained follows: given a grid G and a point $g_{i,j,k} \in G$, it is a characteristic point if:

$$\begin{aligned} IsMajor(x,1,0,0) \;\; AND \;\; & (!IsMinor(x,0,1,0)) \\ AND \;\; & (!IsMinor(x,0,0,1))OR \\ IsMajor(x,0,1,0) \;\; AND \;\; & (!IsMinor(x,1,0,0)) \\ AND \;\; & (!IsMinor(x,0,1,0)) \\ IsMajor(x,0,0,1) \;\; AND \;\; & (!IsMinor(x,1,0,0)) \\ AND \;\; & (!IsMinor(x,0,1,0)) \end{aligned}$$

Where $[1,0,0]$ is the x direction (YZ plane), $[0,1,0]$ is the y direction (XZ plane), $[0,0,1]$ is the z direction (XY plane) and $IsMajor(\cdots), IsMinor(\cdots)$ are predicates which return $TRUE$ if the point is maximum (minimum) in that direction and $FALSE$ otherwise. Figure 1 (a) shows an example of ridge condition for a point p, while Figure 1 (b) shows a point p in the grid which is not a ridge point.

5. Building the mesh

Once all the ridge points have been computed, so that we have identified in the grid G the points in which the probability to be part of the desired surface is more high, we need to build a final triangular mesh, which approximates the desired surface S. Our first idea was to march the cells of the grid, triangulating each triplet of ridge points. Unfortunately, this simple approach leads to not satisfactory results: most of the marked ridges are on the desired surface but some of them are outliers. In order to filter the set of ridges and to improve the result, we decided to implement a method that transfers the information of being a ridge from a vertex to an edge (or more edges) thus achieving sub-voxel precision. This is done with the application of a P-Method (Parabola-Method) which does the following. For each grid point $g_{i,j,k}$ in the grid G and for each principal direction, x, y and z:

1. Take the parabola passing for the EEF values of the grid points $g_{i-1,j,k}, g_{i,j,k}, g_{i+1,j,k}$ (for simplicity, the x direction)
2. Take the maximum max with coordinates (x_max, y_max, z_max) of the parabola (if it exists)
3. Consider the projection of this point.
   - **if** it falls in the interval $[g_{i-1,j,k}, g_{i,j,k}]$ **mark** an *intersection* in this edge;
   - **if** it falls in the interval $[g_{i,j,k}, g_{i+1,j,k}]$ **mark** an *intersection* in this edge.

The P-method is a general smoothing approach which works quite well for large datasets even if some outliers still remain. In any case, at the end of the procedure, we have the intersections in the edges of our grid and we can launch a modified Marching Cubes procedure that starts directly from the intersections instead of the conditions on the vertices of a cell. This procedure definitely improves the quality of the results as it is shown in Figure 2.

6. Implementation and Results

We have tested our method on different datasets [Pap04]. The results of our method on a cube with four supersampled faces and two subsampled faces is shown in Figure 3. From an input dataset of 4240 points (Figure 3(a)), we built

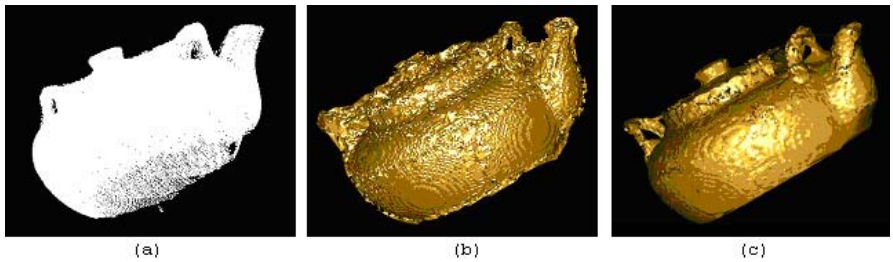

Figure 2: *A teapot: the input dataset (a) shows noisy data especially near the handles. (b) The reconstructed model by extracting the ridge points via the heuristic method (HM) and with no application of the P-method. The model shows noise. (c) The reconstructed model by extracting the ridge points via the heuristic method (HM) and with the application of the P-method. Outliers are eliminated and the model correctly represents the input teapot.*

a grid G of $80x80x80$ grid points. Using an isotropic Gaussian distribution with $\sigma = 0.2$ we obtained 85245 influenced grid points with relative EEF values (Figure 3(b)). Successively, we run the Surface on a Volume method (SVM) obtaining 10245 ridge points (Figure 3(c)) and the Heuristic Method (HM) obtaining 13252 ridge points in less time (Figure 3(d)). The meshes obtained by applying a modified Marching Cubes which starts directly from intersections on edges are showed in Figure 3(e)-(f). Finally Figure 3(g) shows the result of the reconstruction method by the use of the heuristic method (HM) with a filter over the EEF values of the 67%.

The HM method is sensible to symmetries in the object, but it is much faster than the SVM method and, by the use of the filter over the EEF values can reach optimal results on such a simple sampled dataset. On the other hand, the SVM method, using an isotropic Gaussian distribution, is able to reconstruct those faces that are sufficiently sampled, but it is not able to recovery the upper face of the cube that is subsampled (Figure 3(f)).
When dealing with complex input datasets, as in the case of the Stanford bunny and the dragon, the SVM method behaves generally better than the HM method, even if the HM method does not produce as many outliers as in the case of symmetric objects (like the cube above).

Our experiments have shown results which differ by varying some of the modelling parameters we made available in the implemented interface. In particular, the results depend upon:

- the sampling density of the dataset
- the grid resolution
- the sigma vector we are using
- the filter applied on the EEF values
- the approximation error for the ridge condition (only SVM method)

In Figure 4 we show one of our experiment on the Cybeware ball-joint dataset, outlying problems and quality of results with different parameters values,

7. Concluding remarks

We have presented a Surface Reconstruction method that adopts a probabilistic approach and makes explicit use of uncertainty of input samples. This is a first step in the direction of developing a flexible method that can integrate data from different sensors, while exploiting heterogeneous information that can be sensor-specific.

The general framework we have presented is based on an *Estimated Existence Function* (EEF), which is computed incrementally and indicates the probability that the desired surface exists in a particular volume of space. The general idea is that the surface passes through the ridges of such EEF. We have implemented a discrete computation of both the EEF and its ridges on a volume grid, and we have used a variant of the Marching Cubes to extract a surface mesh out of such grid.

While in this paper we have considered just a simple definition of uncertainty, our goal is to integrate more elaborate information that often are made available by sensors, such as uncertainty defined by covariance matrices, and estimation of differential properties of the surface at the sampled points. The idea is that the computational framework remains unchanged, while just the probability distribution function (PDF) is redefined depending on information available. Our current research is aimed at incorporating richer information in the definition of a (more elaborate) pdf and, thus, of the EEF. In the design of new PDFs we will also take into account the need of handling data with variable sampling density. in fact, we found that the EEF used in this paper (which is defined upon a Gaussian PDF), is too sensitive to sampling density.

Experiments presented in this paper are just qualitative and are aimed at exploring the effectiveness of our approach. On the basis of such experiments, the approach seems promising. We have not made, for now, quantitative evaluations (such as computing the maximal, average and minimal errors in reconstruction). This latter issue will be also the subject of our future research.

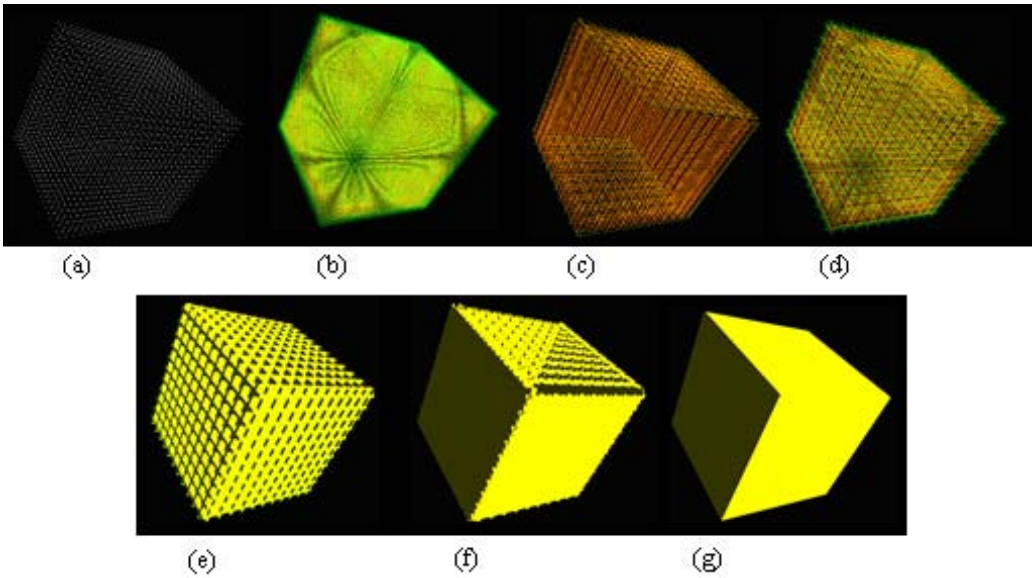

Figure 3: *Application of the both the Surface-on-a-Volume method (SVM) and the Heuristic method (HM) on a cube. An isotropic Gaussian distribution with* $\sigma = 0.2$ *has been used. (a) The initial input points, (b) the EEF function, (c) Ridge points extracted by applying the SVM method, (d) Ridge points extracted by applying the HM method. (e) The reconstructed model from (c). (f) The reconstructed model from (d). (g)The reconstructed model with a filter of* 67% *on the EEF.*

Acknowledgments

This work has been partially supported by the European Commission under the Network of Excellence AIM@SHAPE, contract number 506766 and and by the Italian Ministry of Research and Education under project LIMA3D (Low Cost 3D imaging and modelling automatic system).

References

[ACTL02] AMENTA N., CHOI S., TAMAL K. D., LEEKHA N.: A simple algorithm for homeomorphic surface reconstruction. *International Journal of Computational Geometry and Applications 12* (2002), 125–141. 2

[AS00] ATTENE M., SPAGNUOLO M.: Automatic surface reconstruction from point sets in space. In *EUROGRAPHICS 2000 Proceedings* (2000), vol. 19, pp. 457–465. 2

[Att97] ATTALI D.: r-regular shape reconstruction from unorganized points. In *Proceedings of the ACM Symposium on Computational Geometry* (1997). 2

[BBCS96] BAJAJ C., BERNARDINI F., CHEN J., SCHIKORE D.: Automatic reconstruction of 3d cad models. In *Proceedings of Theory and Practice of Geometric Modelling* (1996). 2

[CL96] CURLESS B., LEVOY M.: A volumetric method for building complex models from range images. In *Computer Graphics: Siggraph Š96 Proceedings* (1996), pp. 221–227. 2

[CM95] CHEN Y., MEDIONI G.: Description of complex objects from multiple range images using an inflating baloon model. In *CVIU* (1995), vol. 61, pp. 325–334. 2

[CMSR00] CIGNONI P., MONTANI C., SCOPIGNO R., ROCCHINI C.: The marching intersections algorithm for merging range images. In *Technical Report B4-61-00* (2000). 2

[EGM*94] EBERLY D., GARDNER R., MORSE B., PIZER S., SCHARLACH C.: Ridges for image analysis. In *Jour. Mathematical Imaging and Vision* (1994), vol. 4, pp. 353–373. 3

[HDD*92] HOPPE H., DEROSE T., DUCHAMP T., MCDONALD J., STUETZLE W.: Surface reconstruction from unorganised points. In *Computer Graphics SIGGRAPH 92 Conference Proceedings* (1992), vol. 26, pp. 71–78. 2

[HSIW96] HILTON A., STODDART A., ILLINGWORTH J., WINDEATT T.: Marching triangles: Range image fusion for complex object modeling. In *Proc. IntŠl Conf. Image Processing (ICIP96)* (1996). 2

[JM02] JOHNSON A., MANDUCHI R.: Probabilistic 3d data fusion for multiresolution surface generation. In *1st International Symposium on 3D Data Processing - Visualization and Transmission* (2002). 2

[JR75] JOHNSTON E., ROSENFELD A.: Digital detection

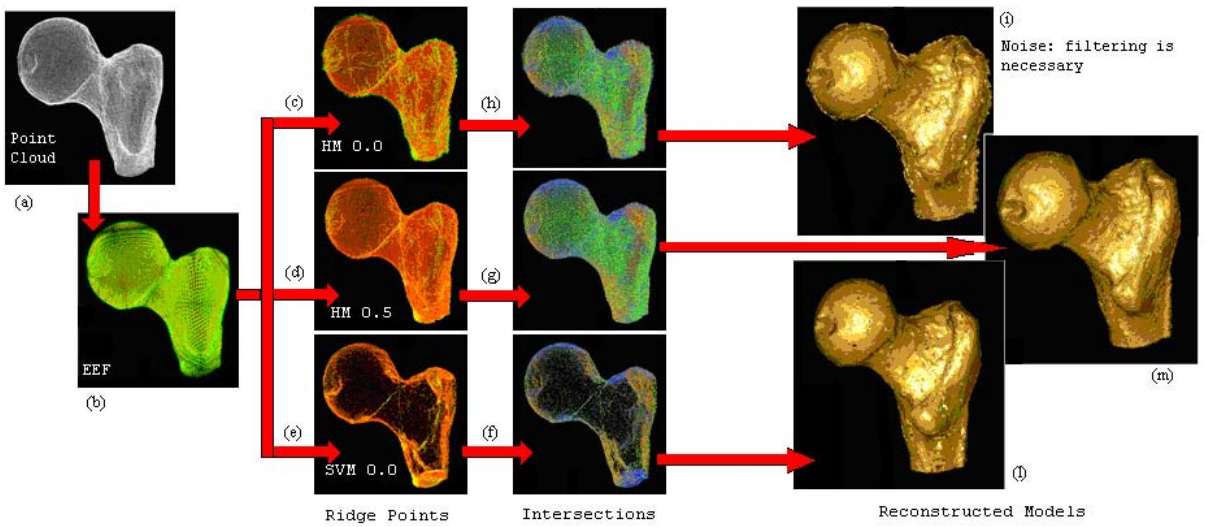

Figure 4: *Three different applications of our method to the cybeware ball-joint dataset: The initial point cloud (a), the computed EEF function (b). Ridge points extracted by applying the Heuristic Method (HM) with no filter on the EEF (c), ridge points extracted by applying the Heuristic Method (HM) with 0.5 filter on the EEF values (d) and ridge points extracted by applying the Surface-on-a-Volume Method (SVM) with no filter in the EEF (e). The intersections (f-h) and the resulting models (i-m).*

of pits, peaks, ridges, and ravines. *SMC 5* (July 1975), 472–480. 4

[Mar83] MARK D.: Automated detection of drainage networks from digital elevation models. In *AutoCarto IV: Proceedings Sixth International Symposium on Computer Assisted Cartography* (1983), p. 288Ű298. 4

[MB95] MONGA O., BENAYOUN S.: Using partial derivatives of 3d images to extract typical surface features. In *Computer Vision and Image Understanding* (1995), vol. 61, pp. 171–189. 4

[MM98] MENCL R., MÜLLER: Interpolation and approximation of surfaces from three dimensional scattered data points. In *EUROGRAPHICS 98 State of the Art Reports* (1998). 2

[Pap04] PAPALEO L.: Surface reconstruction: Online mosaicing and modeling with uncertainty. In *PhD Thesis - Department of Computer Science, University of Genova* (2004), vol. DISI-TH-2004-04. 4

[PMG04] PAULY M., MITRA N. J., GUIBAS L.: Uncertainty and variability in point cloud surface data. In *Symposium on Point-Based Graphics* (2004), pp. 77–84. 2

[Sch01] SCHNEIDER B.: On the uncertainty of local form of lines and surfaces. In *In Cartography and Geographic Information Science* (2001), vol. 28, p. 237Ű247. 2

[Spa99] SPANOS A.: *Probability Theory and Statistical Inference*. ISBN-0521424089. Cambridge University Press, 1999. 3

[SS95] SHIRYAEV A., SHIRIAE A.: *Probability*. ISBN-0387945490. Springer, 1995. 3

[TC98] TEICHMANN M., CAPPS M.: Surface reconstruction with anisotropic density-scaled α-shape. In *Proceedings in IEEE Visualization* (1998), pp. 18–23. 2

[TF78] TORIWAKI J., FUKUMURA T.: Extraction of structural information from gray pictures. *Computer Graphics and Image Processing 7* (1978), 30–51. 4

[TGLW01] TAMAL K. D., GIESEN J., LEEKHA N., WENGER R.: Detecting boundaries for surface reconstruction using co-cones. In *Int. J. Computer Graphics & CAD/CAM* (2001). 2